SAND2018-11421
UNCLASSIFIED UNLIMITED RELEASE
LDRD PROJECT NUMBER: 212041
LDRD PROJECT TITLE: New High-Resolution Electron Scattering Capability
PROJECT TEAM MEMBERS: Jonathan H. Frank, David W. Chandler, Martin P. M. Fournier, Mark J. Jaska

ABSTRACT:

This project explored a new capability for studying collisions of electrons and molecules with unprecedented accuracy by combining high electron-energy resolution with velocity mapped imaging of electrons. Low-energy electrons were produced within a supersonic beam by photoionization of metastable krypton using a dye laser to generate electrons with tunable kinetic energy and a narrow energy spread. A new configuration for electron imaging optics was developed to enable scattering of electrons in a zero-field environment with subsequent rapidly pulsed velocity mapped imaging of the electrons. Development of this new capability will significantly enhance DOE/NNSA's ability to perform basic research on processes relevant to plasmas in atmospheric re-entry and neutron generation for weapons systems and provide fundamental understanding of electron-driven chemistry important to solar energy conversion.

INTRODUCTION:

This Exploratory Express LDRD project provided the initial development of a new apparatus for studying low-energy electron scattering from molecules that is capable of generating electrons with energies between 0.1 and 3 eV at an energy resolution of better than 1 meV. The development of a capability that provides accurate, high-resolution electron scattering measurements will impact multiple programs at Sandia. Sandia has a strong modeling effort to accurately predict the character and species associated with reactive plasmas key to many Sandia missions. Modeling plasma arc, evolution, and reactivity relies on public databases (e.g. www.lxcat.net) that contain experimentally and theoretically determined elastic and inelastic electron scattering cross sections as well as dissociative electron attachment branching ratios. While available databases provide accurate cross sections for certain well-studied systems, reliable cross sections for gases or molecules relevant to Sandia's plasma modeling are limited or non-existent. For some small molecules, available experiments and theory provide reliable total and elastic scattering cross sections, but the understanding of inelastic scattering processes is far from complete [1]. Cross section data for dissociation, ionization, and electron attachment/detachment can be quite limited. The impact of these gaps on plasma models is largely unknown but could be very significant. For example, substantial variations in cross sections for excited states and uncertainties in branching ratios for electron impact dissociation could significantly affect plasma simulations.

Sandia National Laboratories is a multimission laboratory managed and operated by National Technology and Engineering Solutions of Sandia, LLC, a wholly owned subsidiary of Honeywell International, Inc., for the U.S. Department of Energy's National Nuclear Security Administration under contract DE-NA-0003525.

Conventional electron scattering measurements use an electron beam with a monochromator, resulting in relatively coarse energy resolution, limited temporal resolution, and limited information about resonances and branching ratios of electron scattering processes. An alternative approach that overcomes these limitations is to use atomic ionization to produce low-energy electrons [2-4]. The apparatus developed in this LDRD project combines laser formation of low-energy, high-resolution electrons from ionization of metastable atoms and velocity-mapped electron imaging. In velocity mapped imaging, electrons are imaged onto a detector in order to determine the velocity of the scattered electrons and therefore the energy loss during the scattering process. This approach builds on Sandia's extensive expertise in laser diagnostics and ion imaging, which was developed in the laboratory of David Chandler [5].

The project consisted of designing, building, and testing the electron scattering apparatus. The key requirements for the apparatus included the generation of electrons with tunable kinetic energy using laser photoionization of metastable krypton in a supersonic beam, shielding of the nascent electrons from the electric field of an electrostatic lens, and subsequent rapid pulsed acceleration of the electrons to image their velocity distribution. Unlike conventional velocity mapped ion imaging, which operates in a continuous mode, detection of electron scattering requires pulsed operation so that electrons can scatter in a zero-field environment and then be rapidly accelerated onto an imaging detector. The design phase included simulations of electron trajectories for pulsed operation that guided the construction of the electron imaging optics. Experiments successfully demonstrated the formation and imaging of tunable electrons from 0.4 to 0.6 eV by ionization of Kr atoms. After successful formation of tunable electrons, we performed a series of experiments to understand how the apparatus operates under different conditions and to improve the quality of the electron imaging. Subsequent experiments focused on testing the ability to detect electron scattering within a supersonic beam containing a mixture of krypton and molecular oxygen. Electrons scatter elastically from both krypton and oxygen is one process expected to be observed. In addition, vibrationally inelastic scattering is expected by oxygen. This occurs within narrow energy resonances that result from excited states of the O_2^- anion that is temporarily formed upon attachment of the scattered electron [6].

DETAILED DESCRIPTION OF EXPERIMENT/METHOD:

The experiment combines electron generation by laser photoionization of krypton and electron detection by a velocity-mapped imaging (VMI) spectrometer. Figure 1a shows the experimental setup, which consists of a skimmed pulsed supersonic beam, ionization laser, and VMI system. Target molecules are combined with Kr atoms in the pulsed beam, which intersects the laser beam at the focus of the VMI spectrometer. Tunable high-resolution, low-energy electrons are produced by photoionization of metastable Kr, and some of these electrons scatter off the target molecules and krypton atoms in a zero-field environment. Analysis of electron images reveals the final vibrational levels of the molecules from which the electrons scatter and provides a measure of electron scattering cross-sections and branching ratios of different scattering processes.

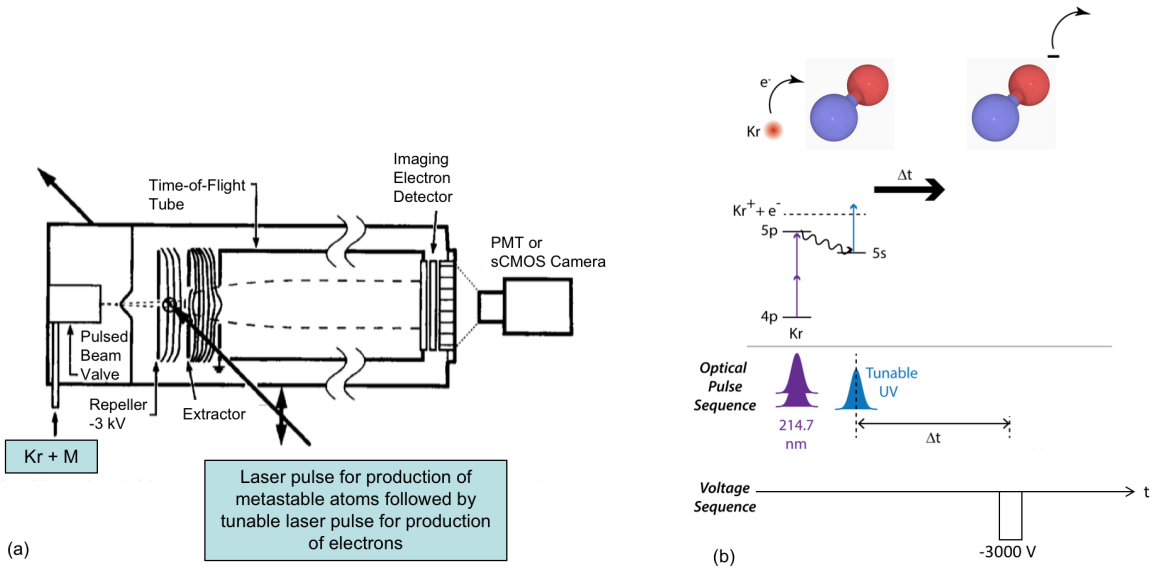

Figure 1. (a) Experimental apparatus for low-energy (0.1-3 eV) electron measurements with high energy resolution of 1 meV. Laser-generated electrons with tunable kinetic energy using ionization of metastable Kr(5s) are combined with velocity mapped imaging photoelectron detection. (b) Timing diagram of the pulsed lasers and electron optics voltages. The first laser pulse populates the Kr metastable state, and the second tunable laser pulse generates electron bursts via ionization of Kr.

The rapid sequence of pulsed lasers and electron optics voltage is shown in Fig. 1b. First, two-photon excitation of Kr at 214.7 nm populates the $5p[3/2]_2$ state at 93123 cm^{-1} [7]. A portion of the excited Kr atoms will fluoresce to the metastable $5s[3/2]^o_2$ state at 79972 cm^{-1}, which has a lifetime of ~45 s. Other electrons will absorb a third 214.7 nm photon and ionize Kr atoms to produce 3.32 eV electrons. Approximately 100 ns later, the metastable Kr(5s) atoms are ionized by a tunable UV laser pulse from the second harmonic of a dye laser with a 3-ns duration and 0.07 cm^{-1} linewidth. The kinetic energy of the resulting burst of electrons is continuously tunable by varying the wavelength of the ionization laser. Kinetic energies up to several electron volts are readily obtained with bandwidths on the order of 1 meV, which is limited by the velocity distribution in the molecular beam and by space charge effects [2]. Within approximately 1-10 ns (depending on the time to traverse the molecular beam), a fraction of these electrons scatter off the target molecules or krypton atoms. A -3 kV voltage pulse is then applied to the repeller plate on the VMI optics to accelerate the electrons through the electrostatic lens and onto a 2D detector. Figure 2 shows the evolution of the resulting electron cloud as it accelerates from the electron production region through a grounded mesh and then through the flight tube onto the microchannel plate (MCP). Secondary electrons produced by the MCP generate signal on a phosphor screen, which is then detected on a scientific CMOS (sCMOS) camera. The electron optics focus the electrons onto the detector, and the resulting image is a 2D projection of the entire electron cloud. The radial extent of the cloud depends on the electron velocities such that electrons with equal velocities are mapped onto the same location on the detector.

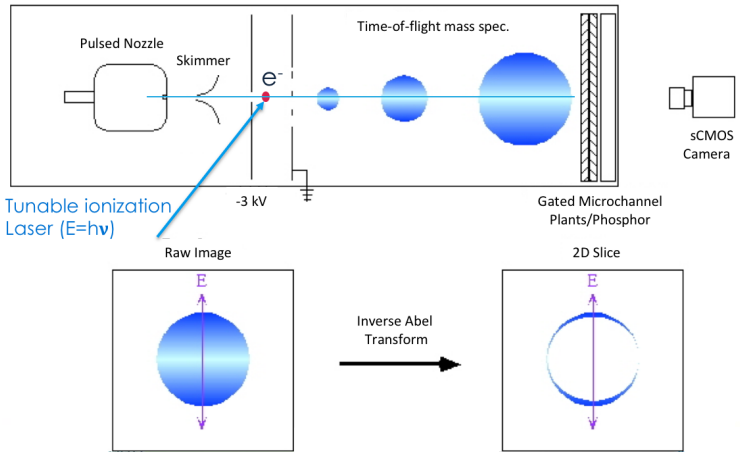

Figure 2. Diagram of velocity map imaging shows acceleration of electron cloud to detector. Recorded image is a 2-D projection of 3-D distribution of electrons from which 3-D velocity distribution can be obtained.

Our existing VMI system is not capable of electron scattering measurements because it uses continuous rather than pulsed voltages. In the continuous wave (CW) configuration, electrons are accelerated by the constant electric field of the repeller and electrostatic lens as soon as they are generated by laser photoionization, resulting in an increase in their kinetic energy. However, electron scattering measurements require the electrons to be generated in a zero-field environment so that no additional kinetic energy is imparted to them after their generation by photoionization. To address this requirement, we developed a new electron imaging configuration that shields the region of electron generation from the continuous electric fields of

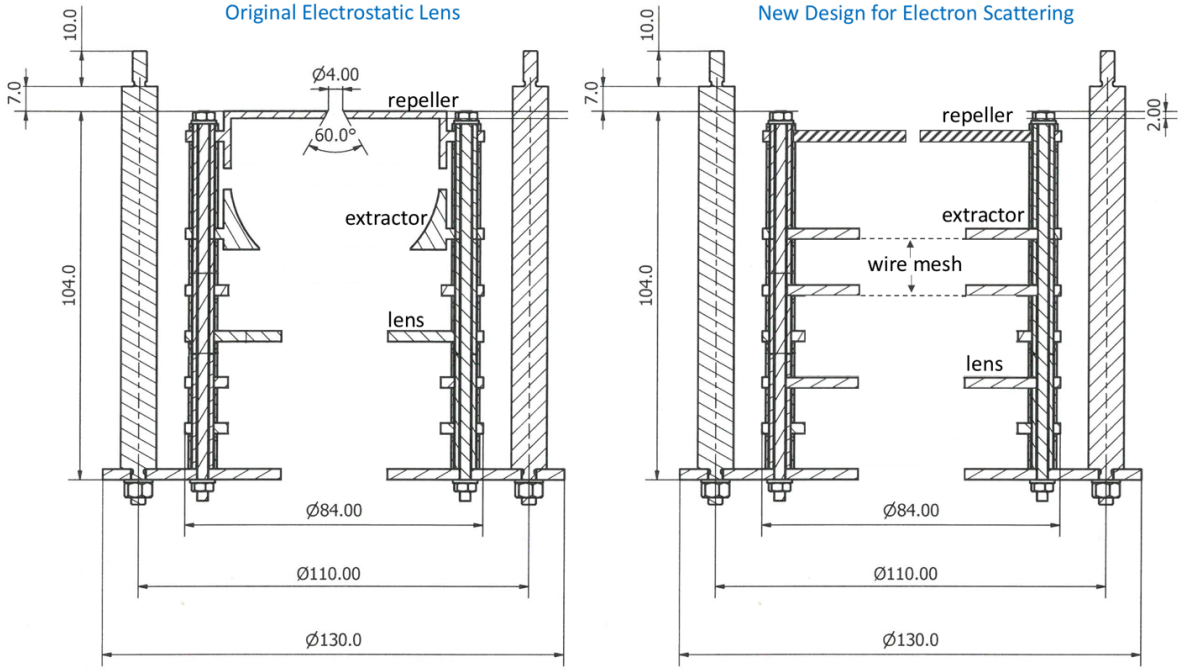

Figure 3. (left) Original electrostatic lens design for CW operation, (right) new design for pulsed operation that is required for electron scattering velocity map imaging.

the electrostatic lens and provides pulsed acceleration of the electrons after they have had several nanoseconds to scatter from molecules in the molecular beam. Figure 3 shows a comparison of the conventional electrostatic optics that are used for CW velocity mapped imaging on the left and the new pulsed VMI design on the right. In the new design, the repeller plate is replaced by a flat plate with a 4-mm diameter hole in the center, and the extractor and adjacent plate are replaced by flat plates with a 30-mm covered by wire mesh. The wire meshes are electrically grounded to shield the region of electron production and scattering from the continuous voltages applied to the electrostatic lens.

RESULTS AND DISCUSSION:

Electron generation from photoionization of krypton

As a first step prior to implementing the pulsed electron optics, we demonstrated the ability to generate a large number of electrons with high energy resolution using photoionization of Kr in an atomic beam using our existing electron imaging apparatus that does not have pulsed fields. Figure 4 shows a velocity mapped image of photoelectrons generated from two different ionization processes. The outer ring of electrons is formed by 2+1 resonance-enhanced multiphoton ionization (REMPI) from the 214.7 nm light, and the inner ring of electrons is formed by 266-nm ionization of the metastable state. The number of electrons produced is limited by charge repulsion that begins to degrade the energy resolution when too many electrons are generated with a single laser pulse. This result demonstrates the well-focused velocity mapped images of electrons with different kinetic energies.

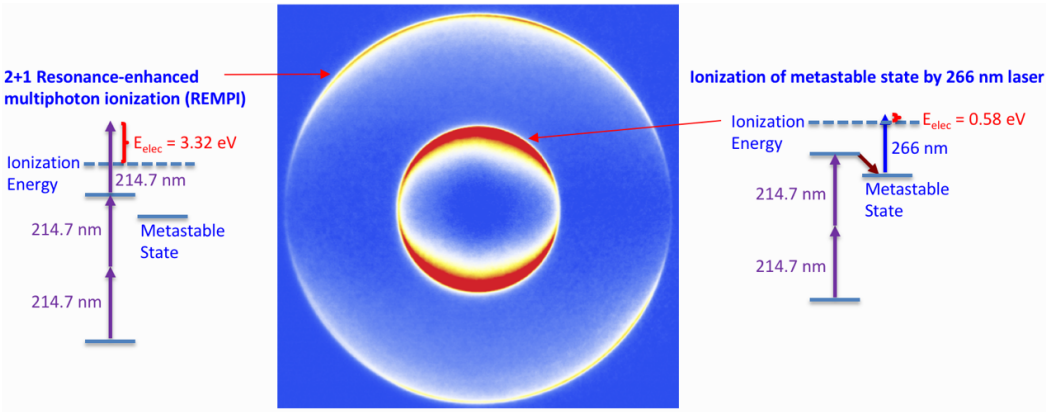

Figure 4. Image of photoelectrons with different kinetic energies (eKE) formed by 2+1 REMPI of Kr at 214.7 nm (outer ring, eKE = 3.32 eV), and by single-photon ionization of metastable Kr(5s) at 266 nm (inner ring, eKE = 0.58 eV).

Imaging of electrons with pulsed velocity mapped imaging

For electron scattering measurements, the design of a pulsed VMI configuration requires the application of a high-voltage pulse to the repeller plate with a duration on the order of nanoseconds such that the pulse ends before any electrons pass through the first wire mesh. This

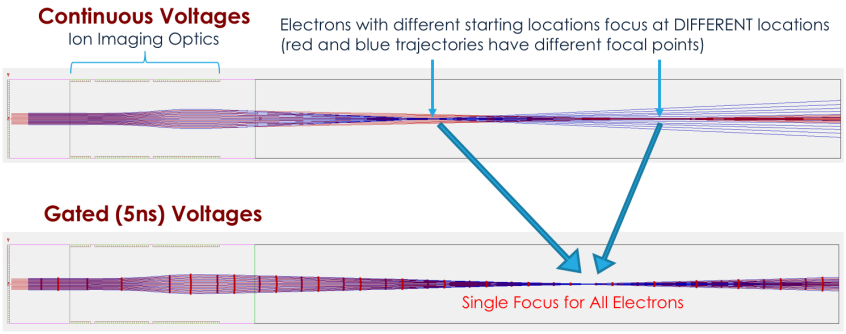

Figure 5. Electron trajectory simulations for continuous and pulsed operation of a three-element Einzel lens show an increased depth of focus for pulsed velocity mapped imaging of electrons.

permits electron scattering to occur in a zero-field environment prior to the application of this high voltage pulse. In addition, all of the electrons are exposed to the electric field of the repeller plate for the same amount of time and therefore experience the same acceleration regardless of their location between repeller and extractor plates. In contrast, the use of a continuous voltage on the repeller plate results in position-dependent acceleration of electrons. In these cases, electrons that are located closer to the repeller are exposed to the electric field longer and are accelerated more than electrons that are located farther from the repeller plate. Consequently, pulsed electron imaging optics can provide a larger depth of field since electrons that originate from different axial locations will be focused at the same image plane, as demonstrated by the electron trajectory simulations in Fig. 5. These calculations for a three-element Einzel lens were performed using SIMION simulation software [8]. The results show that electrons from different origins have different focal planes when continuous voltages are used, but they have a common focus when a short voltage pulse is used instead.

The design of the pulsed VMI configuration was guided by simulations of electron trajectories using the same dimensions as the actual seven-element electron imaging apparatus. Example results of the electron imaging optics simulations are shown in Fig. 6 with a 3D isometric view in the upper panel and a 2D side profile in the lower panel. The entire computational domain is 844 mm long with the majority of the distance consisting of the flight tube with the MCP detector at the end. In practice, the flight tube is surrounded by a mumetal tube that shields the electrons from interference from external fields. The velocity mapping configuration images all electrons having the same velocity onto the same location on the detector. For the simulations in Fig. 6, the pulsed voltage that was applied to the repeller plate was the actual voltage time trace of the pulsed power supply used in the experiments and shown in inset of Fig. 6. The peak voltage was approximately -2900 volts, and the duration of the main pulse was approximately 1.5 ns. In the simulation, six electrons with equal velocities originate from different radial positions separated by 0.5 mm to emulate electrons located at different positions across the molecular beam. The negative voltage pulse on the repeller accelerates the electrons through the two grounded wire meshes. The electrons then enter the electrostatic lens, which consists of three metal plates; a central plate with a 30 mm diameter hole and -211 volts surrounded by two

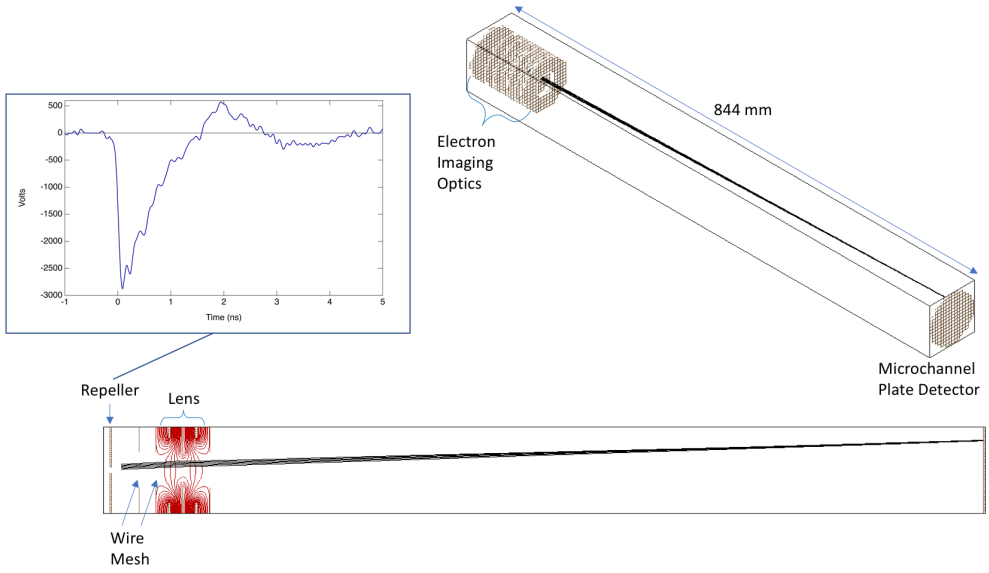

Figure 6. Simulations of electron trajectories (black lines) in newly designed electrostatic lens with a pulsed negative voltage applied to the repeller plate. (top) 3D isometric view, and (bottom) 2D side view with electric field contours (red curves). Inset: Measured waveform from high voltage pulsed power supply that is applied to the repeller plate.

plates with 60 mm holes and 350 volts. The resulting electric field that forms the electrostatic lens is shown by the potential energy curves in the lower figure. The voltages on the lens were adjusted such that the electrons are all focused onto the plane of the MCP, as indicated by the convergence of the electron trajectories at the end of the flight tube.

In practice, the voltage pulse is applied to the repeller plate 3-5 ns after the laser pulse that produces the electrons by photoionization of krypton, which allows sufficient time for 0.6 eV electrons to propagate across the radius of the krypton/oxygen beam. The wire mesh shields this region from the electric fields produced by the fixed voltages on the electron lens, thereby providing a zero-field region for electron scattering to occur prior to acceleration by pulsing of the repeller. To insure the wire mesh provides sufficient shielding for the electrons, we conducted a separate simulation (not shown) of electron trajectories without any voltage applied to the repeller plate. In the simulation, the electrons were initiated with an energy of 0.6 eV and a velocity in the radial direction. In an ideal zero-field environment, the electrons would not experience any acceleration from the electric fields of the electrostatic lens on the other side of the wire meshes. In practice, small electric fields can leak through the wire meshes and impart additional energy to the electrons. The important quantity is the amount of kinetic energy that is imparted during the approximately 5 nanosecond period between electron production by photoionization and electron scattering events. The simulations show that in this short time period, the acceleration of the electrons would be negligible, indicating that meshes provide sufficient shielding of the scattering region.

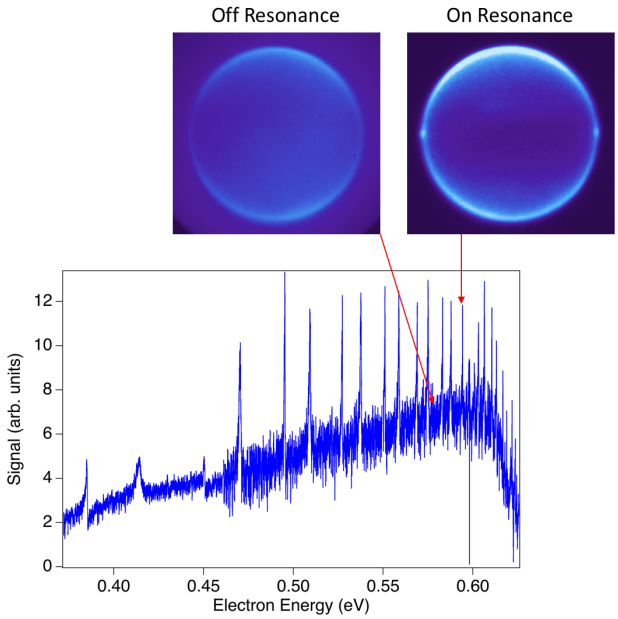

Figure 7. Photoelectron spectrum showing integrated signal for electrons with kinetic energies from 0.35 eV to 0.65 eV with sharp peaks indicating Rydberg states of krypton. Velocity mapped electron images show signals for on and off resonance of the Rydberg states.

After designing and constructing the pulsed velocity mapped imaging optics, we demonstrated their ability to obtain well-focused electron images. The two velocity mapped electron images at the top of Fig. 7 are examples of well-focused images of 0.6 eV electrons generated by photoionization of krypton.

High-energy resolution electron spectrum of krypton Rydberg states

The next critical development step was to demonstrate the generation of electrons with continuously tunable kinetic energies. The electron energy is determined by the energy of the photons that are used to photoionize the excited metastable state of krypton. Electron energies are varied by tuning the wavelength of the dye laser. The minimum tuning step size is comparable to the laser linewidth, which is approximately 0.07 cm^{-1} in the UV, corresponding to approximately 9 ueV. As a demonstration of the tunability of the electron energies, we scanned the wavelength the 266 nm dye laser, which produces electrons with an energy of approximately 0.6 eV, as detected in the velocity mapped images shown in Fig. 7. As the energy was tuned through resonances with Rydberg states of krypton, we were able to detect a significant enhancement in electron production. The spectrum in Fig. 7 shows the integrated signal on the electron images as a function of the electron energy. The narrow spikes in the spectrum indicate significant enhancement in electron generation when the electron energies coincide with Rydberg states of krypton. As the electron energy increases, the energy spacing of the resonances decreases in accordance with the spacing of the Rydberg states. Examples of the velocity mapped electron images for on- and off-resonance conditions are shown at the top of Fig. 7.

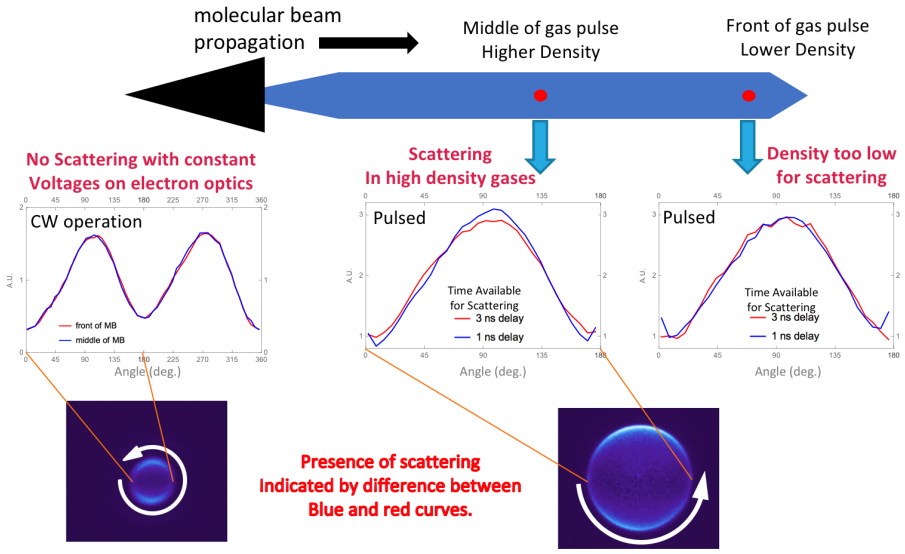

Figure 8. Angular distributions of velocity mapped electron images acquired at different locations in the pulsed gas jet with the front of the jet having lower gas concentration than the middle of the jet. (left) Imaging optics operated in continuous wave (CW) mode; (middle/right) Imaging in pulsed mode with 1 ns and 3 ns delays between the ionization laser pulse and the repeller voltage pulse. Detection of elastic scattering of electrons indicated by broadening of the angular distribution in the middle plot.

Detection of electron scattering

The final development step was to determine the feasibility of detecting electron scattering using the pulsed VMI configuration. To this end, we demonstrated the ability to detect changes in the distribution of the velocity mapped electron images as a result of elastic scattering of electrons. For elastic scattering, the electrons appear at the same radial position in the velocity mapped images since the electron speeds are unchanged. However, the angular distribution changes since elastic collisions change the direction that electrons are traveling. To identify the presence of elastic scattering, we performed pulsed VMI measurements in different regions of the supersonic molecular beam that have different concentrations of gas, as illustrated in Fig. 8. At the front of the gas pulse, the krypton concentration is significantly lower than in the middle of the gas pulse. As a result, electron scattering is expected to be more pronounced in the middle of the gas pulse. The sampled region of the gas pulse is varied by changing the time delay between the pulsed gas valve and the ionization laser.

As a first step, we acquired velocity mapped images of 0.6 eV electrons at the front and middle of the gas pulse using a constant voltage on the repeller plate of the electron optics, as shown on the left of Fig. 8. Each velocity mapped electron image in the figure was acquired by averaging for a half hour with the lasers operating at 30 Hz. The plot above the image compares the angular distribution around the ring of signal in the electron image from the front and middle positions of the gas pulse. The very close overlap of the angular distributions for these two cases indicates that there is no change in the distribution of electron velocities, and consequently no scattering. In the continuous wave (CW) operation of the electron imaging optics, the electrons are

accelerated away from the repeller plate towards the flight tube as soon as they are generated by the ionization laser. Therefore, the electrons formed at low energies do not have sufficient time to scatter before being accelerated to much higher energies for imaging onto the detector. The same measurements were then performed using the pulsed voltage on the repeller plate with 1 ns and 3 ns delay times between the ionization laser pulse and the repeller voltage pulse. The 1 ns delay provides less time for scattering to occur, whereas the 3 ns delay allows sufficient time for the 0.6 eV electrons to traverse the krypton beam and scatter. Differences in the angular distribution of the electron image with the 1 ns and 3 ns delays are indicative of changes in the velocity directions due to elastic scattering of electrons. The overlap of the red and blue curves in the plot on the right of Fig. 8 indicates that there is no scattering detected for the measurements at the front of the gas pulse where the gas concentration is the lowest. In contrast, the middle plot shows a slightly broader angular distribution for the 3 ns delay than for the 1 ns delay, indicating the redistribution of velocities due to elastic scattering. These results demonstrate the feasibility of using the newly developed pulsed velocity mapped electron imaging to detect elastic scattering of electrons in the high-density region of the gas pulse. Future modifications to the VMI system will enable detection of more pronounced differences due to electron scattering as well as inelastic scattering, which has smaller scattering cross sections.

ANTICIPATED OUTCOMES AND IMPACTS:

Electron driven chemistry is all around us. Photosynthesis works by channeling of photon energy to a chromophore where an electron is liberated, and the electron facilitates subsequent chemical reactions by combining with other molecules. Molecular electronics utilize the motion of electrons through conjugated molecular systems. Batteries require electrons to move from a molecule in a solution to a metallic electrode. Plasmas are collections of charged particles (cations, anions, and electrons) and neutral particles and can be either very energetic like an arc or thermalized. This mixture of charged and neutral species can be very reactive and alcohols from methane and ammonia from hydrogen and air have been synthesized in these environments. The study of the individual processes in these complex chemical systems is of fundamental importance for understanding and modeling the systems in a predictive manner.

We have made several innovations in this apparatus that should enable us to perform experiments that others have not been able to do. This apparatus represents the highest resolution electron scattering apparatus anyone has ever built. In order to obtain this resolution, we needed to produce the electrons with high resolution laser radiation and to pulse extract the electrons after they spread and had a chance to scatter. This last innovation of short pulsed electron extraction enables us to image the velocity of the electrons with excellent velocity resolution, and we intend to build on this innovation to produce a more sensitive apparatus.

One issue that we are still struggling with is the residual electrons and ions formed from the first, 214 nm laser beam, that generates the metastable krypton atoms. Some of the atoms are ionized by this laser beam and remain in the molecular beam to form a small plasma since there is no electric field to extract them. Subsequently, the low energy electrons produced by the 266-nm

laser beam can interact with this weak plasma and degrade the energy resolution. When a sufficiently large plasma is present, we observe large variations in the energy distribution of the 266-nm produced electrons. We attempted to disrupt this plasma and extract the electrons by using a pulsed electric field on the first extraction grid. This did not work due to ringing of the electronics that also disrupted our measurement of the low energy electrons. This problem is critical to fix in order to push this technique to its conclusion. We do not see this as a large problem to solve, but it will take some time and ancillary equipment. For now, we have reduced the problem by generating a smaller amount of metastable krypton atoms.

Our newly developed apparatus combines the capabilities of tunable high-resolution electron generation and pulsed velocity mapped imaging setting the stage for studies of electron interactions with a wide range of different molecules. In the limited amount of time associated with this exploratory LDRD, we have only been able to detect elastic scattering. We believe that we need to increase the atomic and molecular density in the beam to detect inelastic scattering. Subsequent work will focus on modifications to the apparatus to enable this density increase. We plan to focus on detection of inelastic scattering of target molecules that are combined in the supersonic jet with krypton as well as observation of dissociative electron attachment. This will require modifications to the present apparatus to bring the nozzle source of the beam closer to the scattering region of the apparatus. The next step will be to observe dissociative electron attachment of CH_3I molecule by low energy electrons forming the I^- anion. Detection of these anions should allow us to further optimize the apparatus.

The ability to measure both inelastic scattering and dissociative electron attachment will enable measurements of quantities important to the modeling of plasmas. The chemistry in plasmas is driven by non-equilibrium chemistry, and that non-equilibrium is generated by electron attachment and detachment from molecules forming vibrationally excited molecules that have enhanced reactivity. This new capability will enable Sandia to better understand the chemistry associated with plasmas and the dynamics of electron transfer within molecules and materials. Development through a full LDRD project could enable electron scattering measurements that are highly relevant to Sandia's programs involving plasmas and couple directly with plasma modelers.

The establishment of a capability for accurate electron scattering measurements is also relevant to a pending DOE/BES proposal on charge localization dynamics using electron attachment/photo-detachment of electrons on large molecules as surrogates for molecular electronics and photosynthetic systems. Electron transport in large molecules drives many processes, and this tool when fully developed will be central to proposals involving these types of systems. Electrons attach to large molecules through diffuse dipole bound states and then evolve into more covalent bound states. Time resolved electron attachment and detachment has the possibility of monitoring in real time this evolution of electron motion within a molecule. We will propose new experiments to DOE utilizing this apparatus.

Built on
LDRD
Laboratory Directed Research and Development

CONCLUSION:

We have successfully built the first prototype low energy electron scattering apparatus with ultra-high energy resolution (< 1 meV) and nanosecond time resolution. We have demonstrated our ability to tune the energy of the electrons from 0.4 eV to 0.6 eV and to image the electrons even after they have spread in space by utilizing a unique pulsed electron extraction technique. We have observed the first elastic scattering signal utilizing this apparatus. The elastic scattering is observed by seeing a change in the angular distribution of the photo-generated electrons. This apparatus still needs to be optimized for the detection of inelastic scattering and dissociative attachment processes. This new apparatus will be central to both LDRD proposals and to DOE Basic Energy Sciences proposals.

Built on
LDRD
Laboratory Directed Research and Development

REFERENCES:

1. Ziółkowski, M., et al., *Modeling the electron-impact dissociation of methane.* The Journal of Chemical Physics, 2012. **137**(22): p. 22A510.
2. Bömmels, J., et al., *Energy broadening due to photoion space charge in a high resolution laser photoelectron source.* Review of Scientific Instruments, 2001. **72**(11): p. 4098-4105.
3. Leber, E., et al., *Vibrational Feshbach resonances in electron attachment to nitrous oxide clusters: decay into heterogeneous and homogeneous cluster anions.* Chemical Physics Letters, 2000. **325**(4): p. 345-353.
4. Schramm, A., et al., *Vibrational resonance and threshold effects in inelastic electron collisions with methyl iodide molecules.* Journal of Physics B: Atomic, Molecular and Optical Physics, 1999. **32**(9): p. 2153.
5. Chandler, D.W. and P.L. Houston, *Two-dimensional imaging of state-selected photodissociation products detected by multiphoton ionization.* The Journal of chemical physics, 1987. **87**(2): p. 1445-1447.
6. Laporta, V., R. Celiberto, and J. Tennyson, *Resonant vibrational-excitation cross sections and rate constants for low-energy electron scattering by molecular oxygen.* Plasma Sources Science and Technology, 2013. **22**(2): p. 025001.
7. Kay, J.J., et al., *Cold atoms by kinematic cooling.* Physical Review A, 2010. **82**(3): p. 032709.
8. *SIMION*. Scientific Instrument Services Inc.: Ringoes, NJ, USA.